Brilliant Yellow, Transparent Pure, and SiO_2-Coated $BiVO_4$ Nanoparticles Made in Flames

Reto Strobel,[†] Hans Joachim Metz,[‡] and Sotiris E. Pratsinis*,[†]

Particle Technology Laboratory, Department for Mechanical and Process Engineering, ETH Zurich, CH-8092 Zürich, Switzerland, and New Technologies, PA Division, Clariant, D-65926 Frankfurt am Main, Germany

Received March 4, 2008. Revised Manuscript Received July 17, 2008

Transparent, yellow bismuth vanadate nanoparticles were made by flame spray pyrolysis. These materials are of special interest as brilliant yellow pigments. The structural properties of the as-prepared powders were characterized by X-ray diffraction, Raman spectroscopy, nitrogen adsorption, transmission electron microscopy, zeta potential measurements, and photospectroscopy. Depending on the particle collection temperature, either pale, amorphous materials or brilliant yellow-green, crystalline $BiVO_4$ with particle size of about 50 nm were formed by direct calcination above 300 °C. The addition of Si during flame synthesis of $BiVO_4$ resulted in smaller such crystals of about 20 nm that were embedded in silica. This prevented sintering of the $BiVO_4$ particles during calcination at 400 °C and resulted in thermally stable, highly transparent, yellow particles.

Introduction

Bismuth vanadates (i.e., $BiVO_4$) belong to a relatively new class of pigments. Their brilliant greenish-yellow color makes them an attractive, nontoxic alternative to lead- and cadmium-based yellow pigments finding applications in paints for automotive and architectural finishes.[1] For coloring of plastics, $BiVO_4$ is thermally stabilized by a dense, multilayer coating of silica or alumina.[1] Transparent pigments with particle sizes smaller than 50 nm could find applications for automotive and industrial coatings, plastics, and inks. Especially, pearlescent and metallic effect pigments require transparent materials which can be achieved by nanosized particles exhibiting low Rayleigh scattering.[2] The applications of $BiVO_4$, however, are not solely limited to pigments as it also exhibits other functionalities such as photocatalytic activity,[3,4] ferroelasticity,[5] and electron conductivity.[6]

Three polymorphs of $BiVO_4$ are known: tetragonal zircon, monoclinic scheelite, and tetragonal scheelite.[5] The monoclinic form exhibits the highest color intensity and is desired for pigmentary applications. Industrially, bismuth vanadates are manufactured by precipitation of sodium or ammonium vanadate and bismuth nitrate[1,7,8] or by solid state reactions.[9] For thermal stabilization, layers of glass-like coatings mainly silicates are added during further processing steps.[1] Regarding transparent $BiVO_4$, Erkens et al.[10] proposed coating precipitated $BiVO_4$ particles with a layer of SiO_2 before calcination to prevent sintering. Additionally, this layer can prevent the photocatalytic activity of $BiVO_4$ in a lacquer as in conventional white TiO_2 pigments.[11] On the other hand, especially the photocatalytic activity of $BiVO_4$ under visible light[4] gave rise to many novel methods for preparation of $BiVO_4$ particles with high surface area. Particles of around 100 nm were prepared by a sonochemical process,[12] whereas a hydrothermal process resulted in 10−40 nm thick sheets of $BiVO_4$.[13] Nanocrystalline materials have also been prepared by intensive ball-milling,[14] sol−gel synthesis,[15] or thermal decomposition of bimetallic Bi−V coordination complexes.[16]

Here, a continuous flame process was developed for synthesis of bismuth vanadate particles.[17] Flame processes are easily scalable and offer a cost-effective method for production of nanoparticles with closely controlled characteristics.[18] Beside traditional flame aerosol synthesis as industrially applied for production of pigmentary titania, flame spray pyrolysis (FSP) is an emerging technology for gas phase synthesis of various nanoparticles for catalysis,[19]

* Corresponding author. E-mail: pratsinis@ptl.mavt.ethz.ch. Phone: +41 44 632 3180. Fax: +41 44 632 1595.
[†] ETH Zurich.
[‡] Clariant.

(1) Endriss, H. Bismuth Vanadates. In *High Performance Pigments*; Smith, H. M., Ed.; Wiley-VCH: New York, 2002; p 7.
(2) Hund, F. *Angew. Chem., Int. Ed. Engl.* **1981**, *20*, 723.
(3) Cherrak, A.; Hubaut, R.; Barbaux, Y.; Mairesse, G. *Catal. Lett.* **1992**, *15*, 377.
(4) Kudo, A.; Omori, K.; Kato, H. *J. Am. Chem. Soc.* **1999**, *121*, 11459.
(5) Bierlein, J. D.; Sleight, A. W. *Solid State Commun.* **1975**, *16*, 69.
(6) Lu, T.; Steele, B. C. H. *Solid State Ionics* **1986**, *21*, 339.
(7) Higgins, J. F. U.S. Patent 4,063,956, 1977.
(8) Wood, P.; Glasser, F. R. *Ceram. Int.* **2004**, *30*, 875.
(9) Köhler, P.; Ringe, P.; Heine, H. German Patent 3,315,851, 1984.
(10) Erkens, L. J. H.; Schmitt, G.; Hamers, H. M. A.; Luijten, J. M. M.; Mains, J. G. E. European Patent 0810269 and U.S. Patent 5,853,472, 1998.
(11) Akhtar, M. K.; Pratsinis, S. E.; Mastrangelo, S. V. R. *J. Am. Ceram. Soc.* **1992**, *75*, 3408.
(12) Zhou, L.; Wang, W. Z.; Liu, S. W.; Zhang, L. S.; Xu, H. L.; Zhu, W. *J. Mol. Catal., A-Chem.* **2006**, *252*, 120.
(13) Zhang, L.; Chen, D.; Jiao, X. *J. Phys. Chem., B* **2006**, *110*, 2668.
(14) Shantha, K.; Varma, K. B. R. *Mater. Sci. Eng., B* **1999**, *60*, 66.
(15) Liu, H. M.; Nakamura, R.; Nakato, Y. *J. Electrochem. Soc.* **2005**, *152*, G856.
(16) Thurston, J. H.; Ely, T. O.; Trahan, D.; Whitmire, K. H. *Chem. Mater.* **2003**, *15*, 4407.
(17) Metz, H. J.; Pratsinis, S. E.; Strobel, R. European Patent 1829825-A1, 2007.
(18) Strobel, R.; Pratsinis, S. E. *J. Mater. Chem.* **2007**, *17*, 4743.

10.1021/cm800622a CCC: $40.75
Published on Web 09/24/2008

as well as for sensors, biomaterials, microelectronics, and even nutritional supplements among other applications.[18] In FSP a combustible liquid precursor solution is dispersed and ignited. After evaporation and combustion of the metal precursors, particles form in the gas phase by nucleation and condensation. Different kinds of materials have already been prepared by FSP processes comprising simple metal oxides, amorphous and crystalline mixed oxides, metals, supported metals, and metal salts.[18] Here FSP was investigated for its potential in preparation of nanostructured bismuth vanadates and $BiVO_4$ embedded in a SiO_2 matrix with focus on structural properties and their influence on color, thermal stability, and transparency.

Experimental Section

Materials Preparation. The experimental setup for synthesis of $BiVO_4$ by FSP has been described earlier.[20] The metal precursor mixture consisted of bismuth(III) 2-ethylhexanoate (72% in mineral spirits, Strem), vanadyl naphthenate (35% in naphthenic acid, Strem), and tetraethoxysilane (>99%, Fluka) for SiO_2-coated $BiVO_4$ powders. These were dissolved in a 1:1 mixture of toluene (>99.5%, Riedel-de Haën) and 2-ethylhexanoic acid (>99%, Riedel-de Haën), resulting in a total metal concentration of 0.4 M (Bi + V + Si). This precursor solution was fed at 5 mL/min through the FSP nozzle by a syringe pump (Inotech) and dispersed by oxygen (5 L/min), forming a fine spray. The pressure drop at the nozzle capillary tip was 1.5 bar. The spray was surrounded and ignited by a small premixed methane/oxygen (1 L/min CH_4, 2.5 L/min O_2) flame ring issuing from an annular gap. Product particles were collected on a glass fiber filter (Whatmann GF/D, 25.7 cm in diameter) with the aid of a vacuum pump (Busch, Seco SV 1040C). The gas temperature in front of the collecting filter was monitored by a thermocouple (K-type) and controlled by varying the distance between the nozzle and the filter (NFD) as shown in Figure 1.

Materials Characterization. The specific surface area (SSA) of the as-prepared powders was determined by nitrogen adsorption at 77 K using the BET method (Micromeritics Tristar). All samples were outgassed at 150 °C for 1 h prior to analysis. The powder X-ray diffraction patterns were recorded with a Bruker D8 advance diffractometer from 10° to 65°, step size 0.05°. The crystallite size of monoclinic $BiVO_4$ (ICSD collection code: 100602) was derived from the corresponding XRD patterns based on the fundamental parameter approach and the Rietveld method using the software TOPAS.[21]

For transmission electron microscopy (TEM), the material was dispersed in ethanol and deposited onto a perforated carbon foil supported on a copper grid. The investigations were performed on a Tecanai 30F microscope (Philips; field emission cathode, operated at 300 kV). The high-resolution TEM (HRTEM) images were recorded on a slow-scan CCD camera.

Raman spectra were measured on a Renishaw inVia Raman microscope using a 785 nm compact diode laser and a CCD detector. Raman spectra were recorded between 100 and 1200 cm^{-1}. Diffuse reflectance spectra were recorded between 300 and 700 nm on a photospectrometer (Varian, Cary 500 Scan) equipped with a powder diffraction cell.

Zeta potentials were measured on a Malvern Zetasizer (Nano ZS) equipped with an autotitrator (MPT-2) to adjust the pH. The as-prepared $BiVO_4$ powders were dispersed in water (Millipore) by ultrasonication, resulting in a concentration of 5 g/L. The pH was adjusted below and above the initial one of the suspension by titration with HCl (0.1 M) and NaOH (0.1 M).

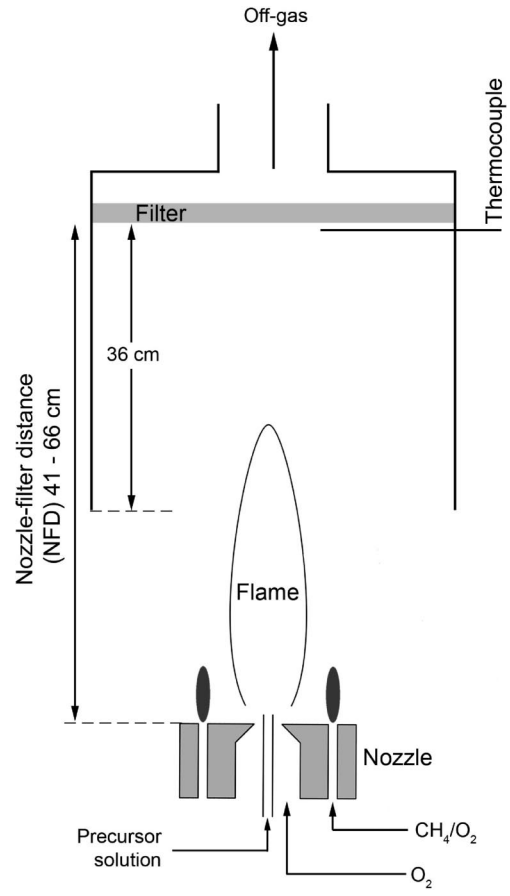

Figure 1. Schematic of the flame spray pyrolysis setup. To achieve different temperatures on the collecting filter, the distance between the spray nozzle and the filter hood (NFD) was varied.

Results and Discussion

Effect of Collection Temperature. Bismuth vanadate has been prepared by FSP and collected on a glass-fiber filter mounted directly over the flame (Figure 1). Typical collection time was around 12 min. Figure 2 shows the evolution of the filter temperature with time at two different filter locations above the burner nozzle. Larger nozzle-filter distances (NFD) resulted in lower maximum filter temperatures (T_f) by dilution of the hot gas stream with the surrounding air. During particle production, the filter temperature increased asymptotically to a maximum, T_f. Figure 3 depicts the influence of NFD on the maximum filter temperature (T_f). When the NFD is increased from 41 to 66 cm, the T_f could be lowered from 362 to 228 °C. The specific surface area of the corresponding particles was strongly affected by the T_f (Figure 3). For T_f < 300 °C the specific surface area was around 35 m^2/g but decreased down to 17 m^2/g for higher T_f.

Figure 4 shows TEM images of $BiVO_4$ prepared at two different nozzle filter distances (NFD) but exactly the same FSP parameters and particle collection time of 12 min. With NFD = 56 cm and a maximum filter temperature of 294 °C

(19) Strobel, R.; Baiker, A.; Pratsinis, S. E. *Adv. Powder Technol.* **2006**, *17*, 457.
(20) Mädler, L.; Stark, W. J.; Pratsinis, S. E. *J. Mater. Res.* **2002**, *17*, 1356.
(21) Cheary, R. W.; Coelho, A. A. *J. Appl. Crystallogr.* **1998**, *31*, 862.

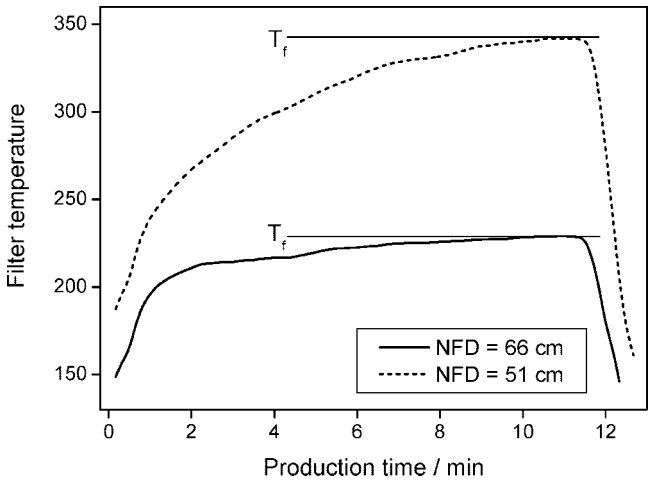

Figure 2. Evolution of the filter temperature during flame synthesis of $BiVO_4$ for two selected nozzle filter distances (NFD). The maximum filter temperature (T_f) is indicated.

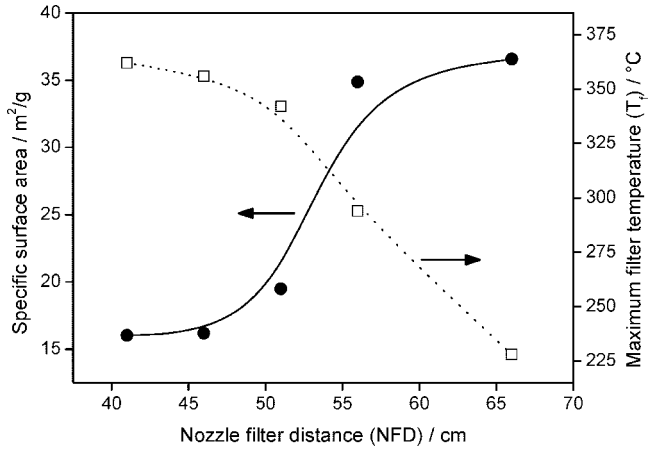

Figure 3. Specific surface area (right axis) of flame-made $BiVO_4$ collected on open face filters as a function of the nozzle filter distance (NFD) along with the corresponding maximum temperature (T_f) on these filters (right axis).

(Figure 4A) small primary particles were formed, whereas at lower NFD (41 cm, 342 °C, Figure 4B) larger particles were observed, consistent with the corresponding specific surface area (Figure 3). Considering the relatively low melting point of $BiVO_4$ (934 °C),[9] the formation of larger particles at high T_f can be attributed to sintering of the collected particles on the filter. The Tammann temperature for $BiVO_4$ can be estimated to be around 300 °C.[22] This, together with associated phase transitions around 300 °C as discussed in the next section, explains the sintering of particles into larger ones at $T_f > 300$ °C.

The T_f affected also the crystallinity of $BiVO_4$. Figure 5 shows XRD patterns of $BiVO_4$ made at different NFD and corresponding T_f. Amorphous materials were formed for $T_f < 300$ °C, whereas crystalline materials were obtained above this temperature in the form of monoclinic $BiVO_4$ (clinobisvanite).[23] Phase pure crystalline monoclinic $BiVO_4$ is also observed by Raman spectroscopy for a powder prepared at high T_f (NFD = 46 cm), exhibiting a Raman spectrum typical for monoclinic $BiVO_4$.[24] This clearly shows that crystallization did not take place in the gas phase but rather on the filter provided that the temperature was high enough. It can be assumed that $BiVO_4$ first forms liquid particles, by nucleation in the flame, that solidify at lower temperatures. However, the very short residence time at high temperatures (a few milliseconds) and the rapid quenching during flame spray pyrolysis[25] do not allow enough time for crystallization, freezing the structure in an amorphous state. If T_f is high enough, particles crystallize after deposition on the filter where the residence time, even of the particles collected toward the end of the production run, is at least 3 orders of magnitude longer (few seconds). A crystallization temperature of about 300 °C is also in agreement with the reversible phase transitions of $BiVO_4$ in this temperature region.[5] The strong increase in particle size above a filter temperature of 300 °C as shown in Figure 3 coincides with the crystallization of the $BiVO_4$ particles. This indicates that sintering on the filter occurs predominately during the crystallization process and is only little affected by slightly higher filter temperature and even less by the collection time (not shown).

The crystallinity of the flame-made materials is also reflected in their color. Figure 6 shows the diffuse reflectance spectra of $BiVO_4$ prepared with low and high T_f at NFD = 56 and 46 cm, respectively. The color of amorphous $BiVO_4$ was pale orange, whereas crystalline $BiVO_4$ exhibited a brilliant yellow-greenish color, characteristic of $BiVO_4$ pigments. The steep decrease in reflectance between 500 and 430 nm is typical for brilliant, yellow $BiVO_4$ pigments.[1] In contrast, the amorphous material exhibited a much flatter profile, reflecting its dull orange color. Additionally, Figure 6 depicts also the above amorphous $BiVO_4$ after its calcination in an oven at 400 °C for 2 h. After calcination the XRD pattern (not shown) of the initially amorphous $BiVO_4$ was the same as that for $BiVO_4$ collected at high T_f. Thus, color and corresponding reflectance spectra were the same for these two materials, independent of where the calcination/crystallization took place (filter or oven).

SiO_2-Coated $BiVO_4$. Flame-made $BiVO_4$ particles were co-oxidized with silica during flame synthesis to thermally stabilize the $BiVO_4$ phase as it is done to stabilize the anatase phase and grain size of TiO_2.[11] In contrast to conventional preparation techniques where such coatings are added after $BiVO_4$ precipitation in a subsequent process step,[1,10] here, coated $BiVO_4$ particles were made in a single step by adding tetraethoxysilane as a SiO_2 precursor directly to the Bi−V precursor solution. All silica-containing powders (5−50 wt % SiO_2) were prepared at low NFD (46 cm) and high filter temperature to ensure direct crystallization on the filter. Figure 7 shows TEM images of as-prepared $BiVO_4$ containing 30 wt % SiO_2. A larger magnification on the right side reveals small $BiVO_4$ crystallites (ca. 20 nm) discernible as darker spots embedded into amorphous SiO_2 (brighter parts).

(22) Knözinger, H.; Taglauer, E. In *Preparation of solid catalysts*; Ertl, G., Knözinger, H., Weitkamp, J., Eds.; Wiley-VCH: Weinheim, 1999; p 501.
(23) Sleight, A. W.; Chen, H. Y.; Ferretti, A.; Cox, D. E. *Mater. Res. Bull.* **1979**, *14*, 1571.
(24) Hardcastle, F. D.; Wachs, I. E. *J. Phys. Chem.* **1991**, *95*, 5031.
(25) Jossen, R. Controlled synthesis of mixed oxide particles in flame spray pyrolysis. Ph.D. Thesis, ETH Zurich, 2006.

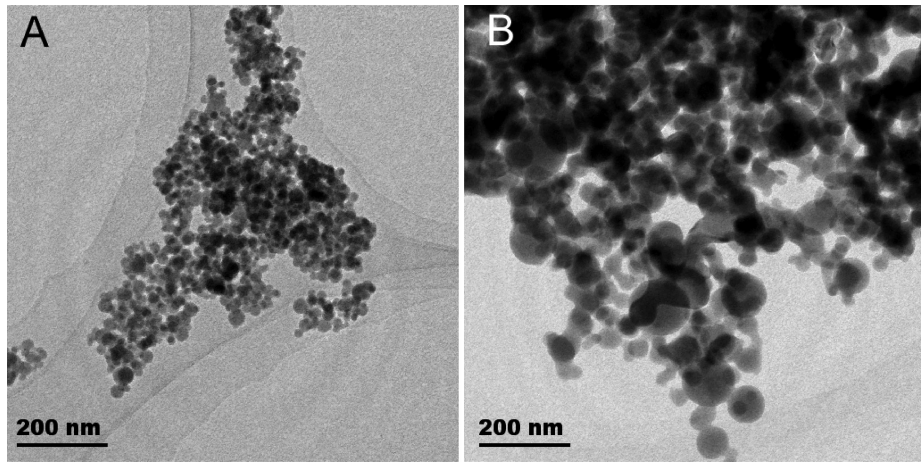

Figure 4. Transmission electron microscopy images of $BiVO_4$ prepared at different nozzle filter distances (NFD). (A) NFD = 56 cm; (B) NFD = 46 cm.

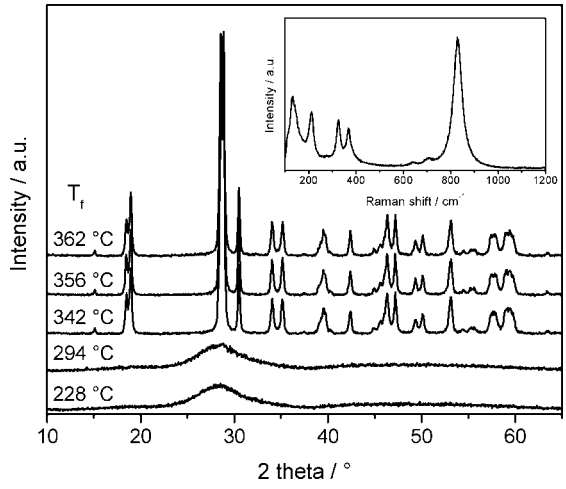

Figure 5. X-ray diffraction patterns of flame-made $BiVO_4$ prepared at different NFD. The corresponding maximum filter temperature is shown on the curves. The inset shows the Raman spectrum of crystalline $BiVO_4$ made at NFD = 46 cm (T_f = 356 °C).

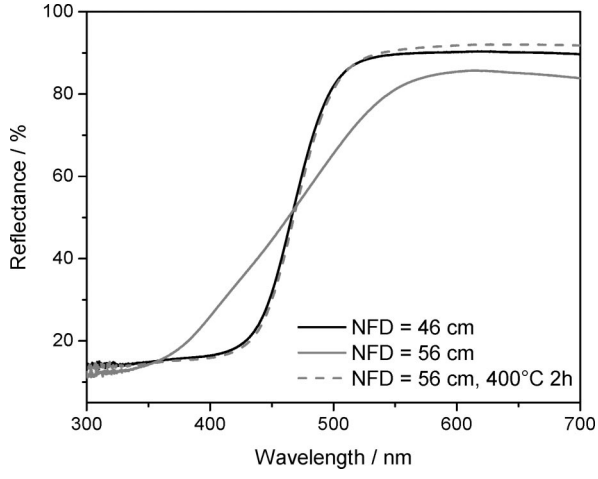

Figure 6. Reflectance spectra of crystalline (NFD = 46 cm) and amorphous (NFD = 56 cm) $BiVO_4$. After calcination and crystallization at 400 °C, the initially amorphous $BiVO_4$ exhibited a spectrum similar to that of the directly crystallized $BiVO_4$.

Zeta potential measurements as discussed later further confirm the formation of SiO_2 around the $BiVO_4$ particles.

On first sight this seems to be surprising as silica exhibits a much higher boiling point (2950 °C) than $BiVO_4$, Bi_2O_3 (1890 °C), or V_2O_5 (1750 °C)[26] and thus should start to nucleate first followed by condensation of Bi and V. However, in the literature it has often been reported that during coflame synthesis of silica with other metal oxides such as TiO_2,[27] Fe_2O_3,[28,29] Ta_2O_5,[30] or ZnO,[31,32] silica tends to coat or embed them. Several mechanisms have already been proposed to explain the coating formation. For vapor-fed flames the coating was either explained by different reaction rates of $SiCl_4$ and $TiCl_4$ toward the corresponding oxides[27] or by differences in the boiling points of the oxides (i.e., V_2O_5/TiO_2), leading to a sequential condensation of the two species with the more volatile species condensing on top of previously formed particles.[33] For the $BiVO_4/SiO_2$ system, however, the latter mechanism can be ruled out as the boiling point of SiO_2 is much higher than the one of the other species. Here, the situation is more complex, as liquid droplets are introduced into the flame, and reaction as well as evaporation rates have to be considered. Faster reaction rates and especially faster evaporation and release from the droplets of the Bi and V precursors could lead to a sequential mechanism with $BiVO_4$ particles being formed prior to SiO_2 that condenses on the $BiVO_4$ particles downstream, forming a coating. Another feasible mechanism has been proposed by Ehrman et al. for Fe_2O_3/SiO_2 and TiO_2/SiO_2[28] and Tani et al. for ZnO/SiO_2.[32] After evaporation and conversion the two components condense together, forming liquid particles. Limited miscibility of the two liquid components and high mobility at the high temperatures leads to phase segregation prior to solidification of the particle. Differences in surface

(26) *CRC Handbook of Chemistry and Physics*, 88 (Internet Version 2008) ed.; CRC Press/Taylor and Francis: Boca Raton, FL, 2008.
(27) Vemury, S.; Pratsinis, S. E. *J. Am. Ceram. Soc.* **1995**, *78*, 2984.
(28) Ehrman, S. H.; Friedlander, S. K.; Zachariah, M. R. *J. Mater. Res.* **1999**, *14*, 4551.
(29) Li, D.; Teoh, W. Y.; Selomulya, C.; Woodward, R. C.; Amal, R.; Rosche, B. *Chem. Mater.* **2006**, *18*, 6403.
(30) Schulz, H.; Mädler, L.; Pratsinis, S. E.; Burtscher, P.; Moszner, N. *Adv. Funct. Mater.* **2005**, *15*, 830.
(31) Mädler, L.; Stark, W. J.; Pratsinis, S. E. *J. Appl. Phys.* **2002**, *92*, 6537.
(32) Tani, T.; Mädler, L.; Pratsinis, S. E. *J. Mater. Sci.* **2002**, *37*, 4627.
(33) Stark, W. J.; Wegner, K.; Pratsinis, S. E.; Baiker, A. *J. Catal.* **2001**, *197*, 182.

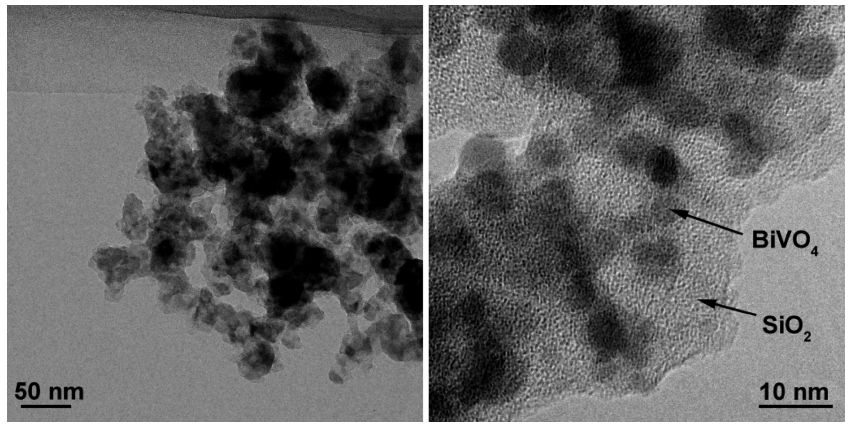

Figure 7. TEM images of FSP-made $BiVO_4$ containing 30 wt % SiO_2. A higher magnification on the right side shows small $BiVO_4$ crystallites (10−20 nm) embedded into an amorphous SiO_2 matrix.

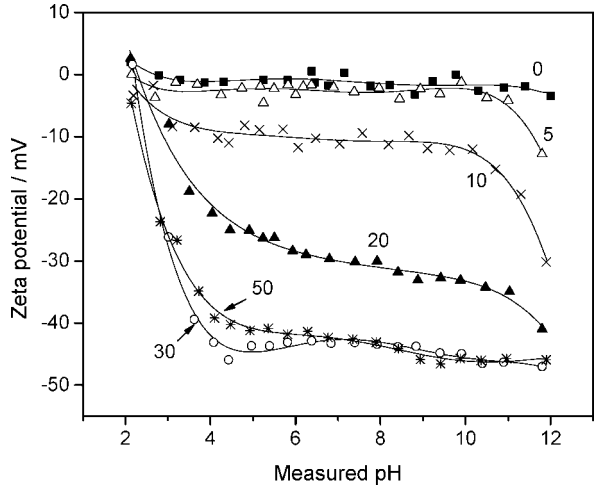

Figure 8. Zeta potential as a function of pH of flame-made $BiVO_4$ containing different mass fractions (wt %) of SiO_2 as marked on the curves.

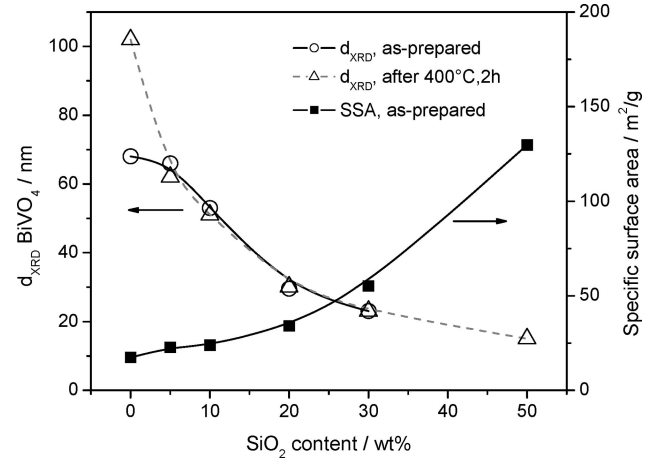

Figure 9. $BiVO_4$ crystal size (left axis) and specific surface area (right axis) of $BiVO_4$−SiO_2 composites as a function of SiO_2 content. Compared to pure $BiVO_4$, the $BiVO_4$ crystallites of the silica-containing powders did not grow during calcination at 400 °C for 2 h.

energy then could lead to the observed enrichment of SiO_2 on the surface during solidification.

Figure 8 shows the zeta potential as a function of pH for $BiVO_4$ with different SiO_2 content. The zeta potential for pure $BiVO_4$ was always around 0 mV over the whole pH range investigated here, indicating the absence of surface charges on the $BiVO_4$ particles. By addition of silica (5−20 wt % SiO_2), the zeta potential changed steadily toward that of pure silica until reaching it at 30 wt % SiO_2. At silica contents higher than 30 wt % the zeta potential was the same as that for pure SiO_2.[34] This shows that the surface density of the Si−OH groups reaches the same value as that for pure SiO_2 when adding 30 wt % SiO_2 and further demonstrates the coverage of the $BiVO_4$ particles by SiO_2 in agreement with TEM (Figure 7). Interestingly, for lower silica contents (5−20 wt %) a drop in the zeta potential could be observed above a pH of 10, which is absent for pure $BiVO_4$ or pure SiO_2. This behavior is most pronounced for 10 wt % SiO_2. It can be assumed that two different surface sites are present at this SiO_2 concentration: One is similar to hydroxyl groups of pure SiO_2 coming from thick SiO_2 layers or particles that exhibit high Brönsted acidity, resulting in a drop of the zeta potential at pH = 3−5. The other, responsible for the decrease above pH = 10, probably comes from a strong interaction of Si sites with $BiVO_4$, resulting in much less acidic hydroxyl groups on the surface that are deprotonated around pH = 10 instead of pH = 3−5.

Figure 9 shows the specific surface area and $BiVO_4$ crystallite diameter for as-prepared and annealed (2 h, 400 °C) materials containing different amounts of SiO_2. The specific surface area increased with SiO_2 content and was not affected by calcination (not shown). More interestingly, the addition of SiO_2 resulted in smaller $BiVO_4$ crystallites with increasing SiO_2 content. Silica acts as a barrier and prevents $BiVO_4$ particles from sintering into larger ones as observed earlier for ZnO/SiO_2.[32] Adding 20 wt % SiO_2 resulted in $BiVO_4$ crystallites of only about 30 instead of 70 nm in pure $BiVO_4$ made at the same conditions.

Amorphous $BiVO_4$ was formed for SiO_2 contents higher than 30 wt %, although the filter temperature was high (NFD = 46 cm, T_f = 350−370 °C), and only after annealing at 400 °C did it transform into crystalline $BiVO_4$. This suggests that SiO_2 impedes the crystallization process. The most significant effect of silica, however, is the stabilization of $BiVO_4$ against sintering at high temperatures. In a comparison of the XRD diameters of the as-prepared and annealed

(34) Gun'ko, V. M.; Zarko, V. I.; Leboda, R.; Chibowski, E. *Adv. Colloid Interface Sci.* **2001**, *91*, 1.

materials, no change could be observed for SiO_2-containing powders. In contrast, pure $BiVO_4$ sintered strongly at 400 °C, increasing its crystallite size from 68 nm up to 102 nm. Even 5 wt % of SiO_2 prevented any such sintering. As the $BiVO_4$ particles are separated by silica from each other, they are not able to sinter as long as the SiO_2 barrier is stable, similar to other flame-made materials that were stabilized by embedding into a SiO_2 matrix.[32]

Conclusions

Yellow bismuth vanadate particles (<100 nm) have been made by single-step flame spray pyrolysis. Depending on the filter temperature where the particles were collected, either amorphous (T_{filter} < 300 °C) or crystalline brilliant-yellow $BiVO_4$ was formed. Silica-coated $BiVO_4$ could also be prepared in one step by adding a Si precursor directly to the Bi−V solution. Especially at silica contents above 20 wt % the $BiVO_4$ particles are completely embedded in a silica matrix as deduced from TEM and zeta-potential measurements. The addition of SiO_2 further quenched $BiVO_4$ particle and crystallite growth and stabilized it against sintering at high temperatures even with just 5 wt % SiO_2, resulting in bright yellow and highly transparent particles.

Acknowledgment. We thank Dr. Frank Krumeich from ETH Zürich for the electron microscopy analysis and the Electron Microscopy Center at ETH Zurich (EMEZ) for providing the necessary infrastructure. Financial support by the Swiss Commission for Technology and Innovation (KTI Grant No. 8316-1) is kindly acknowledged.

CM800622A